Trans. of the Society of Instrument and Control Engineers
Vol.E-5, No.1, 1/10 (2006)

Phased Disaster Data Collection System using Cooperation between Mobile Robots and Spatial Temporal GIS †

Jun-ichi Meguro*, Kiichiro Ishikawa*, Jun-ichi Takiguchi**,
Michinori Hatayama***, Yoshiharu Amano*, Takumi Hashizume*

This paper describes a phased earthquake data collection system using the cooperation between mobile robots and a spatial temporal GIS (Geographic Information System). This proposed method features three-phased data update and models a "change region" as KIWI+ building object data. The 1st update sends the robot position and the omnidirectional images as soon as possible. At the 2nd stage, 3D (three-dimensional) environmental data using the image texture, which is obtained by omnidirectional motion stereo augmented by the RTK (Real Time Kinematic)-GPS/INS, is sent as a VRML format. Finally, the change region, which is recognized by a difference operation between the obtained 3D environmental data and the GIS database, can be recognized as new KIWI+ object data. Field experiments and analyses have proved that the proposed system can provide sufficient data collection/update performance under complicated outdoor environment.

Keywords: Moving Robot, Spatial Temporal GIS, Motion Stereo, GPS/INS, Omnidirectional Vision

1. INTRODUCTION

Collection and assessment of damage information are very important for damage mitigation when large disasters occur. The information of the amount of damage caused by a disaster over a large area is collected by aircrafts and satellites. Moreover, various rescue robots are being developed for local damage-information collection [1)2)]. Moreover, ground/space infrastructure concerning the GPS measurement such as the GEONET (GPS Earth Observation Network System), GPS satellites, and the Quasi-Zenith Satellite System are rapidly maintained; in addition, a high-accuracy RTK (Real Time Kinematic)-GPS, which uses two phase transportation waves, has arrived on the market. Additionally, research and development of a 3D (three-dimensional) GIS (Geographic Information System) is being actively pursued;, and highly accurate GPS and laser radar/camera are installed on a small aircraft and a vehicle and have been used as a mobile mapping system that constructs an elaborate 3D city model [3)4)]. In the future, we can use an ad hoc network even for a disaster situation, which can link wireless self-communication [5)].

In this paper, we propose a phased data collection system using the cooperation between a mobile robot and a spatial temporal GIS [6)], which can connect with disaster management simulator. Additionally, phased data collection experiments were executed using the mobile robot equipped with a highly accurate GPS in order to evaluate the proposed technique.

2. PHASED DISASTER DATA COLLECTION USING MOBILE ROBOT

A. System description

The proposed method consist of a mobile robot that collects the disaster information and a GIS that integrates infornmation (Fig.1). Disaster information should include time information to save disaerved situation transition. We adopt a spatial temporal GIS named "DiMSIS/DyLUPAs," which is useful for the integration of the information collected by various systems, such that both the position and the timestamp of each data are saved in the "KIWI+" format [7)].

The proposed GIS update system comprises three phases. At the 1st update, raw sensor data (e.g., pictures) are updated in real-time in order to have the complete information on the disaster situation. At the 2nd update, the processed sensor data (e.g., a 3D point cloud genereated by raw data) is updated in order to enhance the understanding of the GIS data. At the 3rd update, "change

†This paper was presented at the Trans. of the SICE Vol. 41 No.12 (2005.12)

*Advanced Research Institute for Science and Engineering, Waseda University, 17 kikuicho Shinjuku Tokyo Japan
** Mitsubishi Electric Corp. Kamakura Works, 325 Kamimachiya Kamakura Kanagawa 247-850 Japan
*** Disaster Prevention Research Institute, Kyoto University, Gogajo Uji Kyoto

regions," which are compared with building models stored in a database, are additionally registered as GIS objects in the spatial temporal GIS. The position, posture, and attribute of the change regions are improved for data transportation and general versatility by the 3rd update.

In brief, speedy recognition of a disaster situation is done at the 1st update, and detail information is handled at the 2nd and the 3rd updates. Moreover, the stored information will be connected to another disaster system by using GIS for sharing disaster-damage information with several systems.

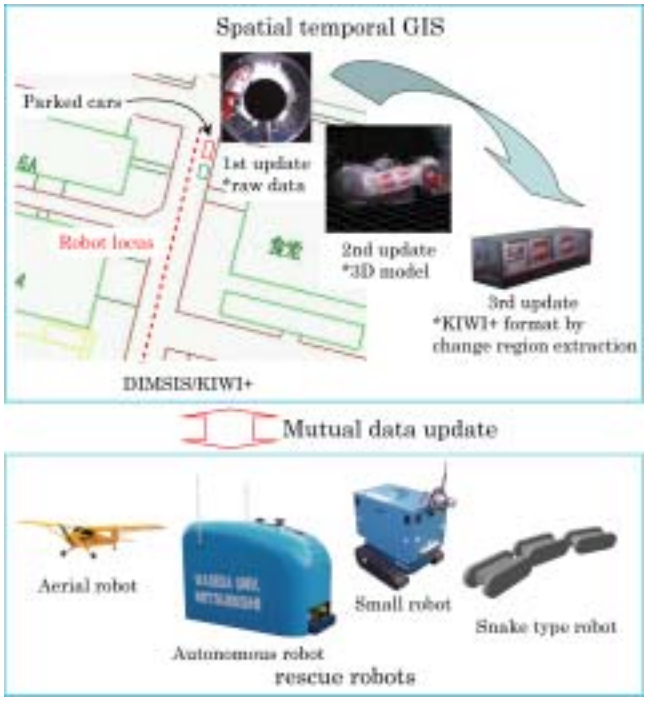

Fig.1 Spatial temporal GIS update method using rescue robots.

B. Development of prototype system

Table 1 shows the sensor configuration and Fig.2 shows the proposed prototype system configuration for phased disaster information update. The proposed system consists of a vehicle and GIS server [7]. The vehicle is equipped with RTK-GPS/INS, which can measure real-time position/posture at several centimeters and 0.1[deg], and an ODV [8], which can capture a 360[deg] color image synchronized with the RTK-GPS/INS update timing [9]. Then, the dense depth map is obtained by motion stereo method using epipolar constraints, which is obtained from a translation and rotation matrix from the RTK-GPS/INS. The Base station consists of DiMSiS/DyLUPAs and a vehicle control terminal. A dense depth map is composed using the GIS building data and change regions such as those occupied by parking vehicles. The change region is finally registered as the object of data KIWI+. A 3D model is generated with the execution of consecutive motion stereo calculation using the time series image captured by ODV and the position/posture information of the change region, which is obtained by the GPS/INS compound operation, and the voting process is applied to the voxel space for the purpose of error reduction and integration of discrete data. This result is compared with the object data in the GIS data server, and a change region (in this research, a road blocked by parking vehicles is considered) can be recognized. The evaluation test is conducted within the enclosure of a factory road (Fig.3).

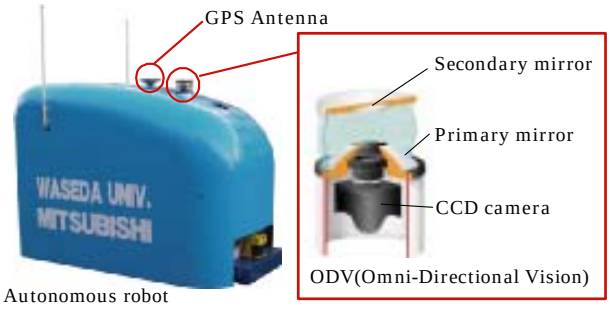

Fig.2 Robot with high-accuracy positioning and omnidirectional vision.

Table 1 Sensor configuration.

Loaded sensor	Product name
GPS Antenna	GeodeticIV (Thales Navigation)
GPS Receiver	Z-Xtreme(Thales Navigation)
MEMS-INS	AHRS400cc-100(Crossbow)
Omni-directional Vision	ODV(Mitsubishi Electric Corp.)

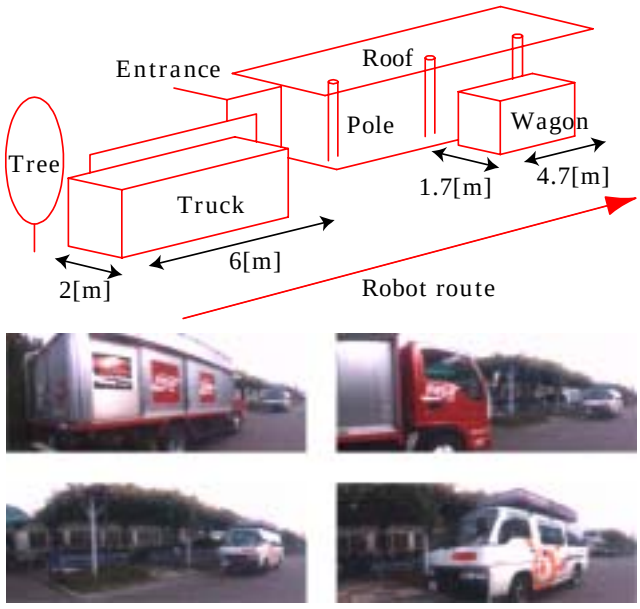

Fig.3 Experiment environment.

3. Speedy Disaster Situation Recognition (1st Update)

In disaster areas, collection and transmission of damage information is expected to be difficult due to damages to infrastructure including telephone lines. Therefore, prompt information collection and transmission becomes the top priority in the early stage of a disaster, regardless of the degree of processing of the information. Formerly, the camera pictures of a disaster area were obtained by persons who then manually updated the data in a GIS by attaching the shooting angle to the picture data. Consequently, neither prompt data update nor automation of the process was attainable. For these reasons, we aim to achieve prompt situation assessment at the 1st update using the robot-collected environmental information. Fig. 4 shows the 1st update data (omnidirectional image, position, posture, and time) in the experiment environment shown in Fig. 3. The raw data of the environmental information are obtained in synchronization with the position, posture, and time data, stored in the chronological order and transmitted to the GIS server. Our system will then update the raw data by integrating it with DiMSIS in accordance with the travel of the robot associated with DiMSIS. In addition, since the system is capable of applying post processing to the stored information, we can also update the data to create panoramic pictures, which are easier for persons to comprehend.

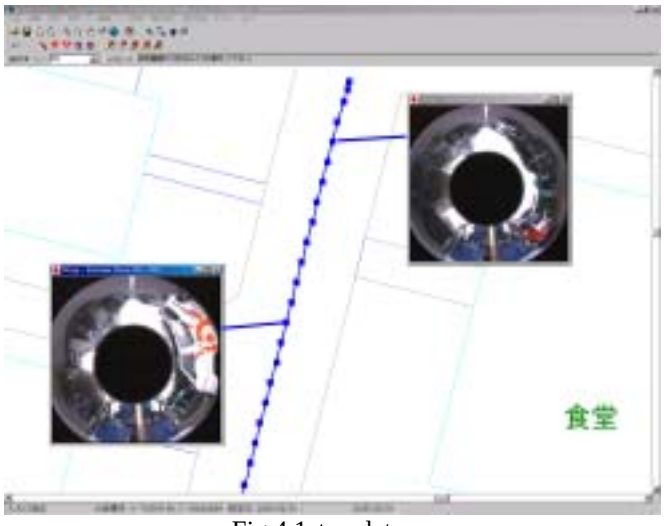

Fig.4 1st update.

4. Detail Disaster Situation Recognition (2nd Update)

A. 2nd update outline

While the 1st update enables prompt situation assessment directly after the occurrence of a disaster, the obtained raw data is unsatisfactory for detailed analysis of a disaster area; therefore, it must be processing in order to visualize it as 3D images. Conventionally, a laser range finder and a camera mounted on a robot have been used to obtain range data and image texture, respectively, which are then combined for further use. However, equipping many disaster area robots with such a group of sensors is impractical in terms of cost-efficiency. For this reason, we propose 3D image reconstruction using the omnidirectional motion stereo technique, which employs an omnidirectional image that can be easily obtained at a low cost using an omnidirectional camera and accurate position and posture data obtained using GPS/INS. By using this method, we create a 3D model using the image texture of the surrounding environment and update the data in a spatial temporal GIS using the 3D model in a VRML format. The visualized 3D data enables us to accurately assess the situation of the disaster area.

B. Omnidirectional motion stereo based on GPS/DR integration

(1) Features of the proposed motion stereo

Motion stereo is a technique used to measure the distance to a particular object by triangulation based on the geometrical information obtained from a single camera. It is characterized by the fact that, as compared to stereo vision using more than one camera, the precision of distance measurement to far objects is increased as the lengths of the baselines can be set arbitrarily and there is no influence from camera alignment errors. However, as the angle of view is small when using a camera with an ordinary angle of view, in order to attain longer baselines, one has to use the camera as if turning around the object to be measured.

In our study, the omnidirectional camera ODV is employed in order to attain a greater amount of disparity between the robot and vehicle in the direction of movement for the purpose of surveillance of the sides of a road. It is possible to attain long baselines in a stable manner as the images on both the right and left sides crossed at right angles to each other in the direction of movement can be obtained by actively using the ODV in motion stereo. Therefore, it is suitable for applications such as mobile robots.

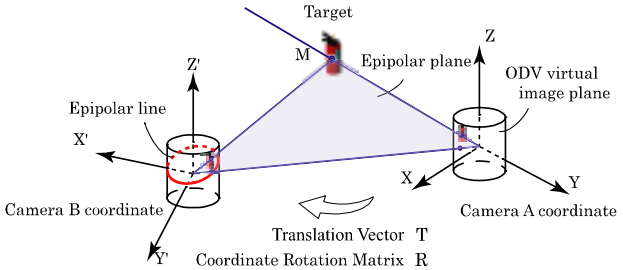

Fig.5 Coordinates of motion stereo.

(2)High-accuracy positioning/heading-angle-based epipolar line calculation

Epipolar lines can be calculated from the amount of camera movement between two images. The ODV coordinates are shown in Fig.6. In this figure, the ODV moves from coordinate A to B with translation matrix T and rotation matrix A. However, it is difficult to calculate the epipolar lines for a doughnut-shaped ODV image field. Fig.7 shows a method of determining the epipolar constraint for the ODV. The point (u, v) on the doughnut image of camera A is transformed into polar coordinates (φ, θ). ϕ_{top} is the vertical angle of view on the upper side; ϕ_{bottom}, the vertical angle of view on the lower side; L_{in}, the distance between the principal point and the innermost circle of the ODV image; L_{out}, the distance between the principal point and the outermost circle of the ODV image; and L_{base}, the distance between the principal point and the base circle of the ODV image. In this study, the equation of an epipolar plane is determined in terms of the relative position and heading angle information of two ODV images. Then, the epipolar lines can be calculated by projecting the intersection line between the epipolar plane and the ODV image plane. The specific method for calculating epipolar lines is explained as follows. First, the coordinate transformation between the digital coordinates of the ODV and the camera coordinates is described. Then, it is assumed that two ODV images with different positions and heading angles are obtained. The polar coordinates are obtained from the equidistant projection of the ODV, as follows:

$$\theta = \tan^{-1}\left(\frac{v}{u}\right) \tag{1}$$

$$\phi = \frac{\phi_{top} - \phi_{bottom}}{L_{out} - L_{in}}(L_{base} - r) \qquad (r = \sqrt{u^2 + v^2}) \tag{2}$$

Hence, in the coordinate system of camera A, M is obtained by transforming from polar coordinates (φ, θ) as follows:

$$M = \begin{bmatrix} X \\ Y \\ Z \end{bmatrix} = J \begin{bmatrix} \sin\phi \\ \cos\phi \sin\theta \\ \cos\phi \cos\theta \end{bmatrix} \tag{3}$$

where J is an arbitrary real number. For example, when $J = 1$, a point on the virtual image plane of the ODV is obtained.

In the coordinate system of camera B, the point, M' that corresponds to point M is given by

$$M' = M[-A][-T] \tag{4}$$

where T and A are the transformation and rotation matrices, respectively (d_x, d_y, and d_z represent the transformation movement and ψ is the heading angle estimated by the GPS/DR). In equation (28), pitch angle, ω, and roll angle, ρ, are included only for the purpose of extensibility; only the heading angle is estimated in this study. However, if a highly accurate three-axis gyro is used, all the angles may be utilized.

$$T = \begin{bmatrix} 1 & 0 & 0 & 0 \\ 0 & 1 & 0 & 0 \\ 0 & 0 & 1 & 0 \\ d_x & d_y & d_z & 1 \end{bmatrix} \tag{5}$$

$$A = A(\psi)A(\omega)A(\rho) \tag{6}$$

O' and M' can be calculated by using the equations (1)~(6). Next, we derive the equation of the plane that includes the three points O', M', and O_2; O_2 is the origin of the coordinate system of camera B. Let us assume that U(x, y, z) is an arbitrary point on the plane. Then, the following equation is obtained:

$$a\overrightarrow{O_2O'} + b\overrightarrow{O_2M'} = \overrightarrow{O_2U} \tag{7}$$

Equation (8) is obtained by eliminating a and b from equation (7). Therefore, any point that satisfies the following equation lies on the epipolar line.

$$\alpha x + \beta y + \gamma z = 0 \tag{8}$$

When point U, which is obtained by transforming digital coordinate $D(u', v')$ in the coordinate system of camera B, satisfies equation (8), D is proved to be the epipolar line. Fig.8 shows an example of the epipolar line of the ODV. The point in the reference image shown in Fig.8(a) corresponds to the circular line in Fig.8(b).

In the SFM method, image feature points are used for calculating the epipolar constraint [11–21]. However, it is generally very difficult to determine feature points in outdoor environments due to the low robustness to complex-background environments. On the contrary, in the proposed method, it is possible to calculate the epipolar constraint even in complex outdoor environments because the information regarding the camera motion is obtained from the GPS/DR, which is not related to the visual environment.

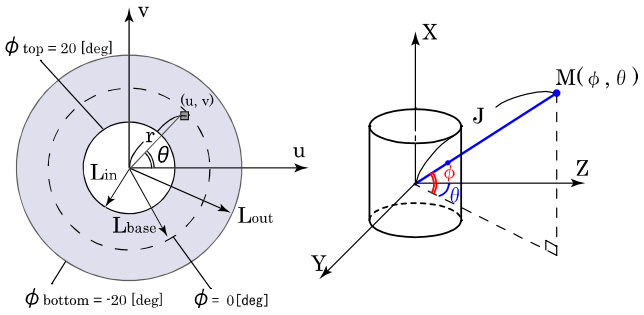

Fig.6 Polar coordinate system transformation.

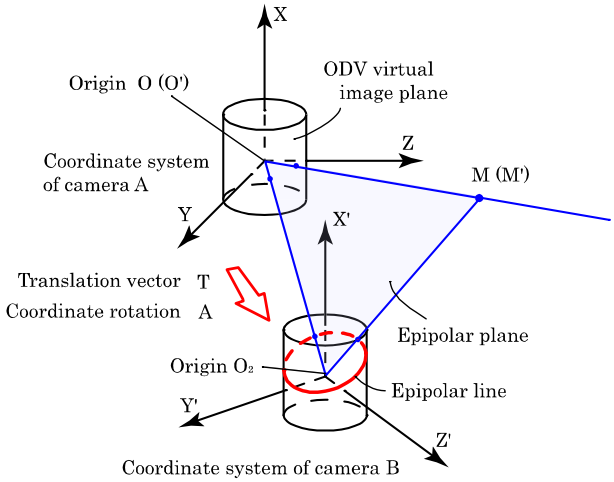

Fig.7 Extraction of epipolar line.

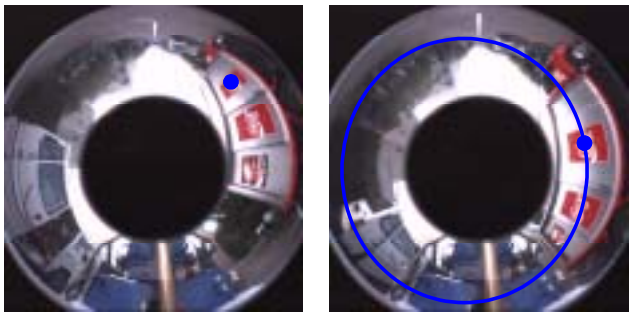

(a) Source image (b) Epipolar line

Fig.8 Epipolar line calculation.

The stereo-matching method estimates distance by triangulation, based on the relationship between two corresponding images. In this method, the reliability of the corresponding points significantly influences the measurement accuracy. Therefore, a robust matching method that combines feature- and area-based matching is presented.

First, color edges are extracted by using a Sobel edge detection filter (Fig.9b). The three primary colors (RGB) are calculated individually to extract these edges. This process determines some potential matching points (Fig.10). Second, color-window matching is applied to these candidate points. Since the search is performed along the epipolar line created by GPS/DR, stereo matching is possible even if the robot moves back and forth and/or from side to side. Third, a window cell ($p \times p$ pixels) is created at some of the candidate points selected by feature-based matching with a reference image, as shown in Fig.11, and is moved along the epipolar line generated by equation (30). In this paper, a rotated square window cell is used. By using each window cell, the RGB-intensity information is matched between both images.

The sum of the differences in the RGB color information of each pixel is given by equations (31)~(34). Here, i and j are the vertical and horizontal coordinates, respectively, of a pixel within a cell at candidate point m. Each pixel has three color values: $red_{(i,j)}$, $green_{(i,j)}$, and $blue_{(i,j)}$. The evaluated value is $E_{(i,j)}$.

Next, I_m is calculated by the SSD (sum of squared differences) method [11]. In the window-matching method, if I_m around the centre of a window is high, matching can be performed with greater accuracy. Therefore, a Gauss distribution is used to weight $I_{m,}$ around the window center. In equation (34), σ is the dispersion. Finally, the minimum, $I_{\min}$, is selected from among the candidate points by feature-based matching.

$$R_{def(i,j)} = \left| R_{base(i,j)} - R_{ref(i,j)} \right|$$
$$G_{def(i,j)} = \left| G_{base(i,j)} - G_{ref(i,j)} \right| \quad (9)$$
$$B_{def(i,j)} = \left| B_{base(i,j)} - B_{ref(i,j)} \right|$$

$$E_{(i,j)} = \max\left\{ R_{def(i.j)}, G_{def(i.j)}, B_{def(i.j)} \right\} \quad (10)$$

$$I_p = \sum_{i}^{w} \sum_{j}^{w} k_{(i,j)} E_{(i,j)}{}^2 \quad (11)$$

$$\mathrm{M} = \min\left\{ I_1, I_2, \cdots, I_p \right\} \quad (12)$$

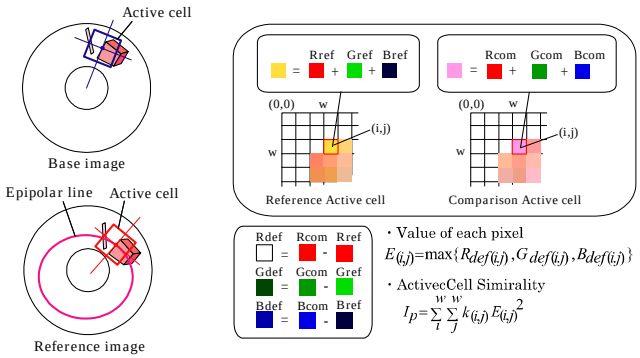

Fig.9 Color window matching algorithm.

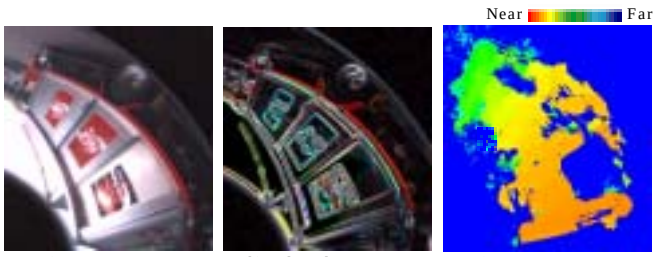

a) Source image b) Color edge image c) Distance image

Fig.10 Distance image calculated by motion stereo.

C. 3D Environment Registration

200 pairs of time series distance image (Fig.15) and the original color images are used for the rendering process, and a t3D model is obtained as shown in Fig.16. It takes about three hours to calculate Fig.16's 3D model by the Pentium4 3-GHz processor. Fig.14 shows the corresponding experimental environment. When Fig.14 and Fig.16 are compared, it can be said that the 3D shapes of the vehicles are excellently well reconstructed.

In order to evaluate the accuracy of the 3D model constructed by the omnidirectional stereo vision (OMSV), first, a data comparison with the data obtained from a laser radar (SICK PLS-101) was performed. Fig.18 shows the histogram of the distance error within a 2–6[m] area. Fig. 17 shows the result obtained from the laser radar and the OMSV, and it can be said that the range estimation accuracy of the OMSV is equal to that of the laser radar. For the OMSV, The standard deviation of the distance error was 151[mm], and it was able to perform a highly accurate distance measurement in the environment with a rich texture.

By using the visualized 3D environmental information, we update the data in the spatial temporal GIS in a VRML format (Fig. 12). Fig. 12 shows that the positions and shapes of parking vehicles can be recognized in detail, which was impossible at the 1st update.

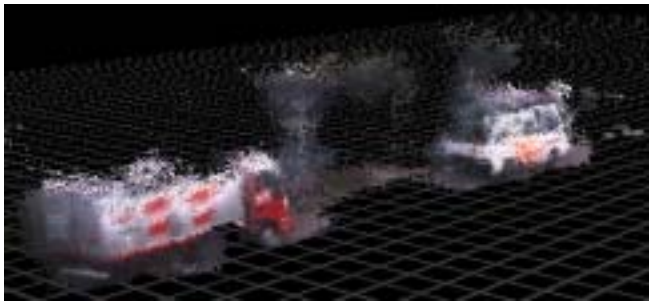

Fig.11 Generated 3D model.

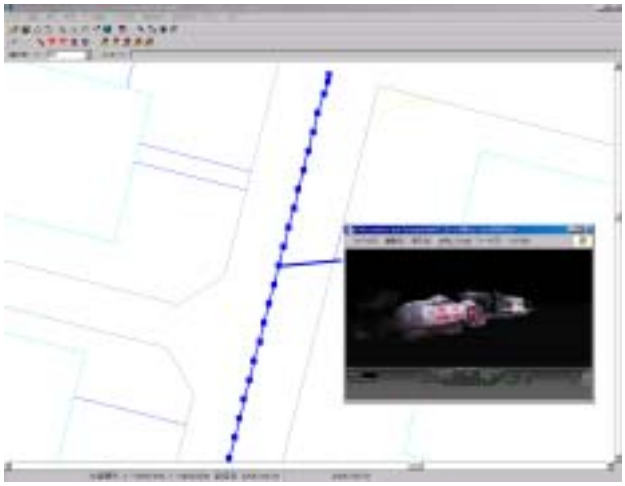

Fig. 12 2nd update.

5. Change Region Registration as GIS object (3rd Update)

A. 3rd update outline

At the 3rd update, our system performs the final processing of the obtained information as a GIS object, which is advantageous in terms of the versatility and processability of data by extracting change regions based on the difference between the reconstructed 3D environment data and the GIS building model obtained in advance. Specifically, the system stores 3D building/road position data as a GIS building object in advance and uses it as the teaching data for the calculation of the difference with the reconstructed 3D environmental data in order to extract change regions by performing a comparison with the conditions before the disaster. Then, the GIS building object in the spatial temporal GIS will be updated only with the change regions in the KIWI+ format. That is, while the update is performed on noncontiguous data (in the VRML format) with color information at the 2nd update and an operator is required to visually check the data one after the other in order to analyze and assess the damages caused by a disaster, the data transmission, compression, and compatibility are improved at the 3rd update since data can be updated in the KIWI+ format by only focusing on change regions; therefore we can expect

that the data connection with superordinate Integrated Earthquake Disaster Simulation System etc. will become easier and enable efficient assessment of the disaster damages for an extensive area.

B. Change Region Recognition

(1)Reference data

In this object recognition, as GIS object data is used as reference, precise 3D environmental data written in absolute coordinates should be registered in advance. Therefore, a precise environmental map of the evaluation field should be measured. More concretely, two sets of area laser radar are mounted on a vehicle and the range data is measured in synchronization with the RTK-GPS/INS update timing. These point data are voted to a 50[cm] × 50[cm] voxel model. Then, the obtained voxel model is converted to surface model and is added with the image texture by a rendering process. The final 3D GIS model is shown in Fig.13. In this model, the absolute position accuracy is 50[cm].

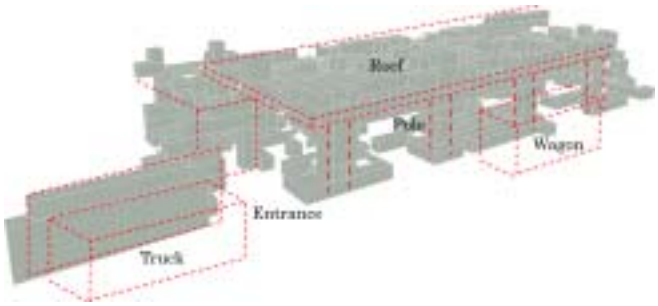

Fig.13 Base voxel model in the experiment environment.

(2)Change Region Extraction

Since this experiment focuses on the surveillance of road blockage conditions, we extract an unknown change region on a road from the reconstructed 3D environmental information using the teaching data. Specifically, we remove the point data corresponding to buildings from the point data shown in Fig. 14(a) using a model of actual environment expressed in 50[cm] polygons and then remove isolated points. The result of the processing is shown in Fig. 14(b). Fig. 14(b) shows that the point data of roadside poles and roofs are removed and only parking vehicles or change regions on the road are extracted. Since there can be multiple objects in the extracted change regions, the regions are classified by object by labeling in order to determine the extent where the object is. In this experiment, objects are classified into two types of parking vehicles.

Finally, we extract surfaces by applying voting process to partitioned grids of the labeled point cloud to create a rectangular model of the change regions. In the example of this experiment, the contour of each surface of parking vehicles is obtained by projecting a point cloud on the distance image onto each of the orthogonal planes X, Y, and Z, as shown in Fig. 15. First, we extract the contour of the top surface of a vehicle from the projected image on the X-Y plane (the top plan view here). Then, we determine the height of the vehicle based on the projected image on the Y-Z plane (refers to the side surface of the vehicle here) and approximate a rectangular solid of the parking vehicle model and calculate the coordinates of each of the eight apexes. Lastly, we extract the texture of each surface of thus obtained rectangular solid from the development image of the ODV and map the texture to the obtained box. Fig. 16 shows the result of this process. Box models are generated corresponding to the point models of a truck and a wagon as shown in Fig. 16(a) and the vectors composing the boxes are expressed by longitude and latitude as shown in Fig. 16(b) and the image texture on the sides of the box will be updated.

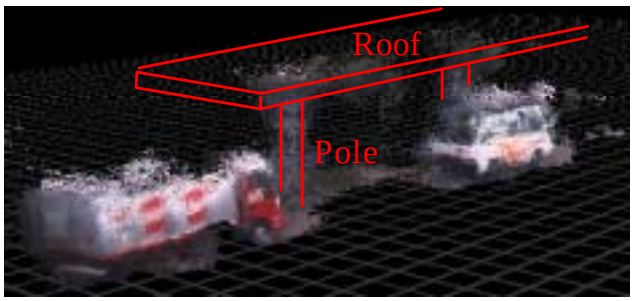

a) Generate 3d model

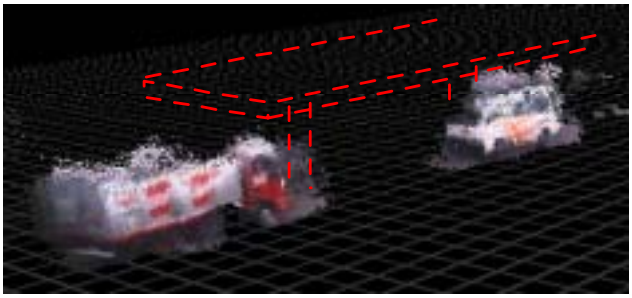

b) Change region extraction

Fig.14 Extraction of difference between 3D model and GIS.

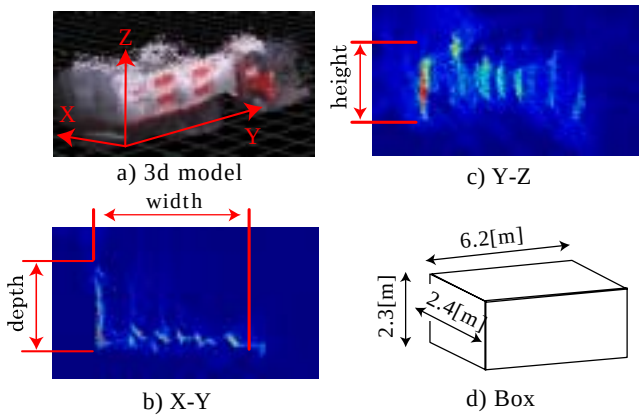

a) 3d model c) Y-Z

b) X-Y d) Box

Fig.15 Generating box by voting range dates.

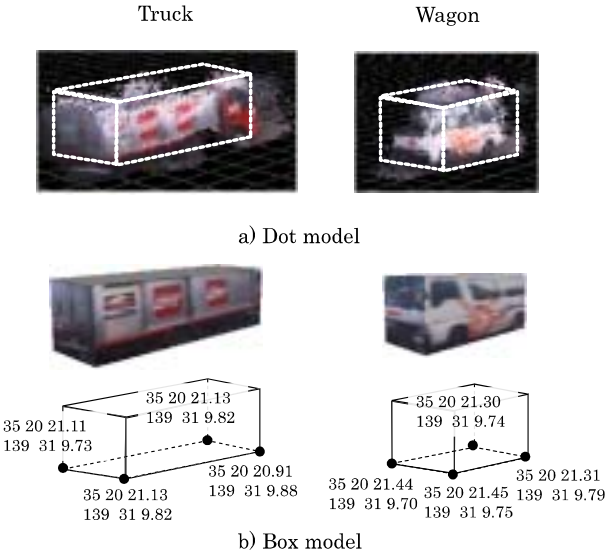

a) Dot model

b) Box model

Fig.16 Surfaces recognition result.

C. GIS update as KIWI+ object

This experiment aimed to recognize parking vehicles on a road, which are not in the GIS data, and update the GIS data with the change region data, particularly to assess the road blockage conditions. The result of updating the data in the Temporal Spatial GIS with the “change regions” is shown in Fig. 17. From this figure, it can be seen that the GIS data are updated with the data of parking vehicles as the change region data. The 3rd update enables to use detailed information including position, posture, and attribute of the changed object in a GIS format, which is advantageous in terms of the versatility and transmission of data as well as to effectively update data in/connect to the Integrated Earthquake Disaster Simulation System, a superordinate system, contributing to an enhancement in the simulation accuracy and efficient assessment of damages over a large area. In addition, the processing time, including the 2nd update, is expected to be within an acceptable and a practical range (about half a day) if we consider the future improvement in the computer processing speed and the introduction of parallel processing as well as employment of hardware system. This is because, for damage assessment, our system is intended to be used not immediately after a disaster but after a certain period of time has elapsed.

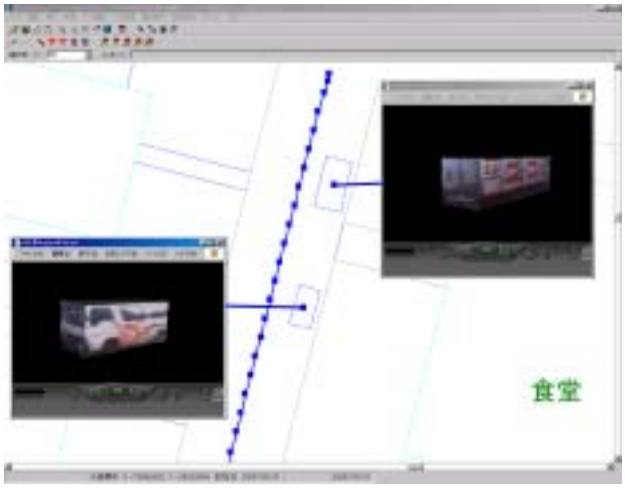

Fig.17 3rd update.

6. Conclusion

In this paper, we proposed a phased information collection method that employs a robot equipped with a group of sensors to achieve prompt and accurate information collection, which is required in the early stage of integrated earthquake disaster simulation in a countermeasures headquarter established at the time of disaster. The proposed method of updating the earthquake data is characterized by a three-phase data update in order to achieve both (1) prompt collection/transmission and abstraction of damage information and (2) extraction and update only of change region data among the earthquake damage data obtained by a robot as building data in a KIWI+ format. Specifically, we first perform prompt assessment of damages, which is required immediately after the occurrence of a disaster, at the 1st update using the raw data obtained from the sensors, which are low in the degree of processing. Then, we successively transmit more detailed information with higher degree of processing of the data at the 2nd and the 3rd updates in order to update the data in aspatial temporal GIS. In this way, we can achieve both the freshness of the data required in the early stage of disasters and the versatility and workability of the data, which enable the data also to be used for post-processing such as integrated earthquake simulation.

In an evaluation experiment using a prototype system, we have run a robot equipped with GPS/INS and an omnidirectional camera on a road in a factory premise,

which simulated a disaster area and performed update only of self-posiiton and omnidirectional image at the 1st update. At the 2nd update, we obtained 3D environmental information using the omnidirectional motion-stereo technique. Then, at the 3rd update, we extracted a change region based on the differences between the reconstructed latest 3D environmental information and the GIS building model obtained in advance and approximated rectangular solids of unknown objects, which have changed due to an earthquake, and updated the DiMSIS data with the change data as a KIWI+ object. We have thus demonstrated that the 3rd update enables us to describe the detailed information on the position, posture, and attribute etc. of changed objects in a GIS format, which is advantageous in terms of the versatility and transmission of data, and the method boosts the convenience for effective connection to a superordinate system, Integrated Earthquake Disaster Simulation System, and efficient assessment of damages over a large area.

7. ACKNOWLEDGEMENT

We would like to thank Dr. Kakumoto (National Research Institute for Earth Science and Disaster Prevention) and the Nagata ward office for experimental support. This research work was supported by the Special Project for Earthquake Disaster Mitigation in Urban Areas (DDT project) sponsored by the Ministry of Education, Culture, Sport, Science and Technology, Japan.

References

1) H. Nakanishi, et al, Robust Control System Design by Use of Neural Networks and Its Application to Autonomous UAV Flight Control, Proc. Of the 2004 Int. Joint Conf. on Neural Network, 2004

2)F. Takemura, et al, Proposition of a human body searching strategy using a cable-driven robot at major disaster, Int. Conf. of Robots and Systems(IROS), , pp.1456-1461, 2004

3)C. Fruh, et al, Automated Texture Mapping of 3D City Models With Oblique Aerial Imagery, 2nd International Symposium on 3D Data Processing, Visualization, and Transmission (3DPVT), 2004

4)R. Shibasaki, et al, A New Interface for Extracting Urban Spatial Objects using Vehicle-borne Laser and CCD Cameras, Proc. of Computers on Urban Planning and Urban Management ,2003

5)I. Noda, M. Hatayama, Common Frameworks of Networking and Information-Sharing for Advanced Rescue Systems, Int. Conf. of Robotics and Biomimetics (ROBIO), 2004

6)M. Hatayama, S. Kakumoto and H. Kameda: Development of Dynamic Management Spatial-temporal Information System and Application for Census Data - Toward Asian Spatial Temporal GIS (ST-GIS) (2)-, Proceedings of Dynamic and Multi-Dimensional GIS, IAPRS, Vol.34, Part2W2, pp.123-127, 2001.

7)J. Meguro, et al, Autonomous Mobile Surveillance System based on RTK-GPS in Urban Canyons, Journal of Robotics and Mechatoronics (JRM), No.17 vol2

8)A.Takeya, et al.,"Omnidirectional Vision System Using Two Mirrors", Novel Optical Systems Design and Optimization SPIE Vol.3430, pp.50-60, 1998

9)R. Hirokawa , et al, Autonomous Vehicle Navigation with Carrier Phase DGPS and Laser-Scanner Augmentation, ION GNSS 2004

10)J. Meguro, et al, Omni-directional Motion Stereo Vision based on Accurate GPS/INS Navigation System, Workshop on Integration of Vision and Inertial Sensors (InerVis2005)

11)N. Yokoya , 3-D modeling of an outdoor scene from multiple image sequences by estimating camera motion parameters, Proc. 13th Scandinavian Conf. on Image Analysis(SCIA2003), pp. 717-724, July 2003

12)K. Yamazaki, et al. 3-D Object Modeling by a Camera Equipped on a Mobile Robot, Proceedings of the 2004 IEEE International Conference on Robotics and Automation (ICRA2004), pp.1399-1405, April 2004

Jun-ichi Meguro（Member）

He received his B.Eng and M.Eng degrees all in Waseda University in 2003 and 2005. He is a graduate school student at Waseda University, and JSPS Research Fellow since 2006. He interests in Unmanned Vehicle Systems, GPS technology and Geographic Information Systems.

Kiichiro Ishikawa

He received his B.Eng and M.Eng degrees all in Waseda University in 2004 and 2006. He is a graduate school student at Waseda University. He interests in Mobile Mapping system.

Michinori Hatayama（Menber）

He recieved his M.Eng in control engineering from Osaka University in 1994 and D.Eng from Tokyo Institute of Technology in 2000. He has been an associate professor in Disaster Prevention Research Institute, Kyoto University since 2005. He joined Japan Digital Road Map Association from 2000 to 2002 and Laboratory for Safety Analysis, Swiss Federal Institute of Technology(ETH) in 2006 as a guest researcher. His current research interests lie in spatial temporal geographic information systems, rescues support systems, and disaster risk management support system.

Jun-ichi Takiguchi

He received his B.Eng, M.Eng and D.Eng degrees in Waseda University in 1984, 1986 and 2004. Since 1987, he has been working at Mitsubishi Electric Corporation Kamakura Works in the field of guidance, control. And then, he also received M.Se degree form University of Edinburgh in 1998. Since 2006, he has been an Visiting Associate Professor of Waseda University.

Yoshiharu Amano

He received B.Eng., M.Eng., and Dr.Eng. in control engineering from Waseda University in 1991, 1994 and 1998 respectively. He has been a Research Associate, a Visiting Lecturer and then an Assistant Professor in Waseda University. He is an Associate Professor in Waseda University from 2002. He is interested in analysis and optimization of power and energy systems. Member of SICE, JSME, ASME, etc.

Takumi Hashizume（Menber）

He received his B.Eng, M.Eng and D.Eng degrees in Waseda University in 1974, 1976 and 1980. He has been a Research Associate, a Lecturer, an Assistant Professor and then an Professor in Waseda University. He is an in Waseda University from 1987. He is interested in power and energy systems.